Human Molecular Genetics, 2009, Vol. 18, No. 21 ***4171–4179***
doi:10.1093/hmg/ddp368
Advance Access published on July 31, 2009

Tbx22^{null} mice have a submucous cleft palate due to reduced palatal bone formation and also display ankyloglossia and choanal atresia phenotypes

Erwin Pauws[1], Aya Hoshino[1], Lucy Bentley[1], Suresh Prajapati[2], Charles Keller[2], Peter Hammond[1], Juan-Pedro Martinez-Barbera[1], Gudrun E. Moore[1] and Philip Stanier[1,*]

[1]UCL Institute of Child Health, 30 Guilford Street, WC1N 1EH London, UK and [2]Greehey Children's Cancer Research Institute, The University of Texas Health Science Center, San Antonio, TX, USA

Received May 29, 2009; Revised and Accepted July 29, 2009

Craniofacial defects involving the lip and/or palate are among the most common human birth defects. X-linked cleft palate and ankyloglossia results from loss-of-function mutations in the gene encoding the T-box transcription factor TBX22. Further studies show that *TBX22* mutations are also found in around 5% of non-syndromic cleft palate patients. Although palate defects are obvious at birth, the underlying developmental pathogenesis remains unclear. Here, we report a *Tbx22*^{null} mouse, which has a submucous cleft palate (SMCP) and ankyloglossia, similar to the human phenotype, with a small minority showing overt clefts. We also find persistent oro-nasal membranes or, in some mice a partial rupture, resulting in choanal atresia. Each of these defects can cause severe breathing and/or feeding difficulties in the newborn pups, which results in ~50% post-natal lethality. Analysis of the craniofacial skeleton demonstrates a marked reduction in bone formation in the posterior hard palate, resulting in the classic notch associated with SMCP. Our results suggest that *Tbx22* plays an important role in the osteogenic patterning of the posterior hard palate. Ossification is severely reduced after condensation of the palatal mesenchyme, resulting from a delay in the maturation of osteoblasts. Rather than having a major role in palatal shelf closure, we show that *Tbx22* is an important determinant for intramembranous bone formation in the posterior hard palate, which underpins normal palate development and function. These findings could have important implications for the molecular diagnosis in patients with isolated SMCP and/or unexplained choanal atresia.

INTRODUCTION

Cleft palate (CP) is a common birth defect with an incidence of 1 : 1500 (1). CP may present either as an isolated congenital abnormality or in association with other clinical features, as part of a syndrome (2). Submucous cleft palate (SMCP) forms a clinically important sub-group, which may be at least as common as overt CP, with a reported incidence of 1 : 1250 (3) to 1 : 5000 (4). SMCP can be characterized as bifid uvula, a notch in the posterior hard palate and/or palatal muscle diastasis (5). In the latter, the palatine muscle inserts incorrectly onto the hard palate causing velopharyngeal insufficiency (VPI) (6). Whether muscle diastasis is caused by a defect in palate myogenesis, by a malformation of the posterior palatal bone, or both is currently not clear. When one or more of the characteristic anatomical features is present without VPI, the term occult SMCP is sometimes used. SMCP-related VPI is considered part of the clinical spectrum of CP and is a common cause of feeding difficulties, speech problems and otitis media-related hearing loss.

Human *TBX22* encodes a T-box protein containing transcriptional repressor activity and is mutated in X-linked cleft palate and ankyloglossia (CPX; MIM303400) (7–10). CPX is an X-linked semi-dominant craniofacial disorder affecting male patients and approximately one-third of female carriers (7). Ankyloglossia without a CP is seen in many carrier females and occasionally in males, indicating a partial penetrance (8,11). Similarly, a detectable ankyloglossia is not always present in CPX patients who are affected by a CP.

*To whom correspondence should be addressed. Tel: +44 2079052867; Fax: +44 2079052832; Email: p.stanier@ich.ucl.ac.uk

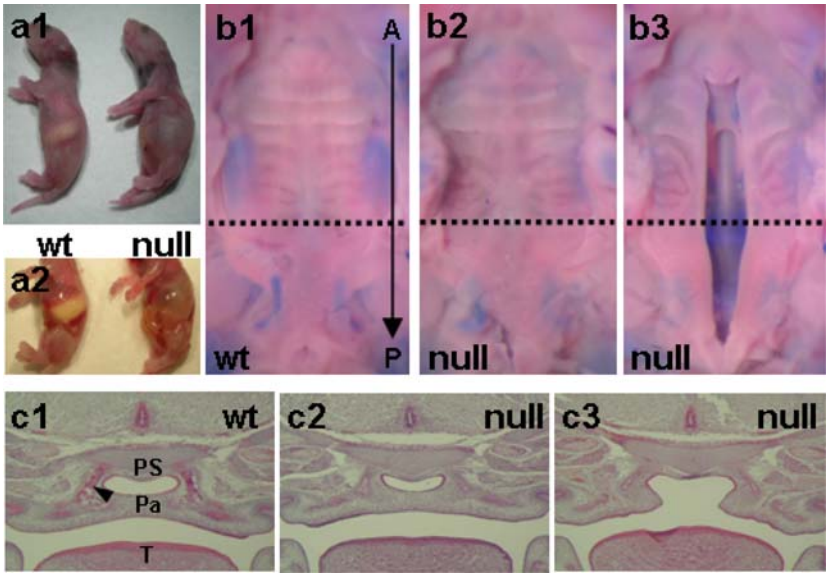

Figure 1. *Tbx22*^{null} mice show submucous cleft palate. (**A**) Approximately 50% of mutant animals die within 24 h post-partum, exhibiting breathing problems and inability to suckle. Their overall anatomy is grossly normal but with air rather than milk in the stomach. (**B**) Male hemizygous *Tbx22*^{null} (−/Y) and female homozygous animals (data not shown) are affected, displaying submucous (b2) or overt (b3) clefts. SMCP can be identified by the irregular and more widely spaced location of the rugae. (**C**) Submucous or overt cleft palate can be observed in E15.5 coronal sections through the posterior end of the hard palate (dotted line). Bone mineralization (pink osteoid) can be seen in the lateral parts of the wild-type fused palate (arrow), while in the SMCP and CP mice, ossification is severely reduced. Pa = palate, PS = pre-sphenoid, T = tongue, A = anterior, *P* = posterior.

In general, there is high inter- and intrafamilial phenotypic variation which ranges from ankyloglossia alone, SMCP, bifid uvula or cleft of the soft and hard palate, all with or without ankyloglossia (7–9,12). Loss-of-function mutations include frame shift, splice site and nonsense mutations, along with missense changes which have been shown to impair DNA binding and sumoylation (13). Sequence variation in the *TBX22* promoter has recently been associated as a risk factor for CP, but predominantly in patients with ankyloglossia (14), although coding region mutations are also found in 4–8% of non-syndromic cases of CP (8,9).

TBX22 is part of the TBX1 sub-family and shares a close evolutionary origin with TBX15 and TBX18 (15). Members of this gene family (*Tbx1*, *Tbx15*, *Tbx10*, *Tbx18* and *Tbx22*) are all expressed in the craniofacial area, and mutation of *Tbx1* and *Tbx10* results in CP phenotypes (16,17). Additionally, haploinsufficiency of the *TBX1* gene is the major gene responsible for DiGeorge syndrome, where one of the features is CP (DGS; MIM188400). Expression of *Tbx22* in mouse and chicken is seen in the posterior palate, caudal tongue, nasal mesenchyme, extra-ocular mesenchyme (Supplementary Material, Fig. S1) and early somites (12,18,19). This pattern correlates well with the phenotypic characteristics found in CPX patients but suggests additional roles for TBX22 in development. Although the defects associated with mutations in *TBX22* are obvious at birth, the underlying developmental pathogenesis remains unclear.

Here, we have created a *Tbx22*^{null} mouse, which has a SMCP, similar to the human phenotype. In addition to ankyloglossia, we find oro-nasal defects including choanal atresia. The latter defect causes post-natal lethality in ∼50% of mutant mice. Analysis of the craniofacial skeleton demonstrates a marked reduction in bone formation of the vomer and in the posterior hard palate, resulting in the classic notch associated with SMCP. Ossification is severely reduced after condensation of the palatal mesenchyme, resulting from a delay in the differentiation and/or maturation of osteoblasts. Rather than being involved in palatal shelf closure, we show that TBX22 is a major determinant for intramembranous bone formation in the posterior hard palate, which underpins both normal palate development and function.

RESULTS

Generation of mice lacking *Tbx22*

To study the molecular and cellular pathogenesis of CPX, we disrupted mouse *Tbx22* by gene targeting (Supplementary Material, Fig. S1). In brief, we introduced loxP sites flanking the first three exons to create a floxed line. *Tbx22*^{flox} animals did not show any phenotypic abnormalities. Subsequently, we removed the first three exons, including the start codon, the N-terminal repression domain, nuclear localization signal and part of the T-box domain, using a βactin-Cre deleter strain to create a *Tbx22*^{null} allele. This allele was bred onto a CD1 background. After initial inspection of *Tbx22*^{null} embryos (homozygous *Tbx22*$^{-/-}$ females or hemizygous *Tbx22*$^{-/Y}$ males) at embryonic day (E) 18.5 no palatal phenotype was immediately obvious. However, we then noticed a Mendelian imbalance in the survival of *Tbx22*^{null} pups after birth. Approximately 50% of these animals struggle to breathe and/or fail to suckle effectively resulting in death within 24 h. The stomach and intestine were filled with air rather than milk (Fig. 1A), similar symptoms to those described for other mouse models of CP (e.g. *Tgfb3*^{null}) (20). Close inspection of the orofacial morphology of

Tbx22^{null} embryos, showed an aberrant pattern of rugae in the posterior half of the hard palate, combined with an area of translucency in the posterior portion (Fig. 1B). A small number of *Tbx22*^{null} embryos (2/30) were identified with an overt CP (Fig. 1B). Detailed analysis of the secondary palate at E15.5 revealed that although fusion along the entire anterior–posterior axis was complete, the posterior hard palate was affected by severely reduced bone formation in all of the mutants analyzed ($n = 30$). This is illustrated by the lack of ossified bone matrix in haematoxylin and eosin (H&E) stained coronal sections of mutant compared with wild-type embryos (Fig. 1C).

Anomalies of the craniofacial skeleton

At E18.5, skeletal preparations of *Tbx22*^{null} mutants stained for bone and cartilage show an abnormal palatine process of the palatal bone and an under-developed vomer although the surrounding craniofacial skeleton is normal (Fig. 2). The palatine process provides the skeletal contribution to the posterior hard palate while the vomer sits anterior and rostral to the palate and is the supporting structure for the nasal cartilage and the secondary hard palate. The scale of bone loss can be seen in the bone surfaces generated from microCT scans of E18.5 embryos (Fig. 2B and Supplementary Material, Movies S1–S6). The mutant vomer is reduced in size and has not fused in the midline. Posterior palatal bone has formed in the dorsal–ventral direction but has not progressed in the lateral–medial direction. The total size of the vomer and palatine process is reduced by 74% (vomer) and 68% (palate) ($n = 4$). Together, these results are consistent with a SMCP phenotype.

Palatine bone deficiency results from a reduction in osteoblast maturation

To investigate the molecular mechanisms involving TBX22 in craniofacial development, we examined the expression of a number of genes known to play roles in palate development such as *Pax9*, *Snail*, *Msx1*, *Msx2*, *Bmp4*, *Osr1* and *Tgfb3*. With the exception of *Pax9* (discussed below) and a modest increase of *Msx2* in the posterior tongue, no significant differences in the levels or patterns of expression were detected in the developing craniofacial tissues of *Tbx22*^{null} embryos (Supplementary Material, Figs S2 and S3). Next, we investigated whether the resultant effect of TBX22 loss on palatine bone formation was through interference with the osteogenic process. Close inspection of coronal sections of the head at E15.5 shows a region of condensed mesenchyme in the mutant, but a complete lack of mineralized bone, as opposed to the wild-type control (Fig. 3A). This result implies that the impaired ossification is a direct result of osteoblasts failing to mature in the *Tbx22*^{null} mutant. Alkaline phosphatase activity, a marker for osteoblast activity is significantly reduced in the mutant palate, indicating that osteoblasts do not reach a mature enough status where they are capable of bone mineralization (Fig. 3B). The alkaline phoshatase activity in control sections shows that osteoblasts have differentiated and are actively involved in the ossification process. Although normal activity can be seen in the mutant's mandible, forming around Meckel's cartilage (Fig. 3B) and at anterior regions of the secondary palate (data not shown), only very low activity could be observed in the developing posterior palate.

To determine the effect of TBX22 loss on osteoblast differentiation, we analyzed the expression of *Runx2*, an early determinant of the osteoblast lineage from mesenchymal cells (21) in mutant animals. No difference in *Runx2* expression was observed at E13.5 between mutant and wild-type posterior palates (Supplementary Material, Fig. S3), while at E15.5 differences reflect the poor development of the bone matrix in *Tbx22*^{null} mutants (Fig. 3C). The area of expression is clearly smaller than the condensed mesenchyme weakly expressing alkaline phoshatase, indicating a reduced number of differentiated osteoblasts. Expression of *Runx2* in E15.5 *Tbx22*^{null} posterior palate resembles the *Runx2* expression pattern in E14.5 wild-type embryos (data not shown), indicating a delay of at least 1 day.

Tbx22^{null} mice have ankyloglossia and choanal atresia

Further comparative histological analysis of craniofacial structures between wild-type and *Tbx22*^{null} mouse embryos revealed a more anterior caudal attachment of the tongue to the mandible (Fig. 4A). This is similar to the shortened frenulum, frequently seen in human CPX patients with ankyloglossia. This feature was consistent in all mutant animals studied ($n = 30$), but does not extend to the tip of the tongue, representing a mild form of ankyloglossia. Another defect, this time not expected based on known CPX phenotypes, was choanal atresia. The choanae are located at the anterior end of the medial nasal prominence allowing air to flow from the nasal cavity into the oral pharynx, reaching the trachea. However, in *Tbx22*^{null} embryos, a persistent oro-nasal membrane (Fig. 4B), which narrows or blocks this passage, restricts nasal breathing. This defect is clearly illustrated in microCT scans of E18.5 embryos (Supplementary Material, Fig. S4). In severe cases, the choanae are blocked along their entire anterior–posterior length, although in milder cases only the posterior part of the choanae is obstructed. It is likely that the anterior position of the membrane will have a marked effect on the survival of the newborn pups. The most severe cases are incapable of nasal breathing, causing gasping for air and making suckling impossible for affected pups (Fig. 5A). Indeed, an investigation of *Tbx22*^{null} newborn pups suggests that the choanal phenotype is likely to be the main cause of the post-natal lethality. Choanal atresia was absent in all of the surviving male null animals analyzed but present in those that suffered a premature demise (Fig. 5B). In older, weaning stage animals, we observed that surviving mutants had a persistent notch in the posterior hard palate (Fig. 5C) indicating the SMCP, but with normal choanae. At E13.5, *Tbx22* expression is clearly detected in the medial and lateral nasal mesenchyme at the site where the oro-nasal fins occur (Supplementary Material, Figs S1 and 5D). In wild-type, *Pax9* expression overlaps in this region with *Tbx22*, although in the mutant the expression is both upregulated and the domain enlarged to span across the persistent oro-nasal membrane (Fig. 5D). These data are consistent with a possible role for PAX9 in the timely rupture of the oro-nasal membrane.

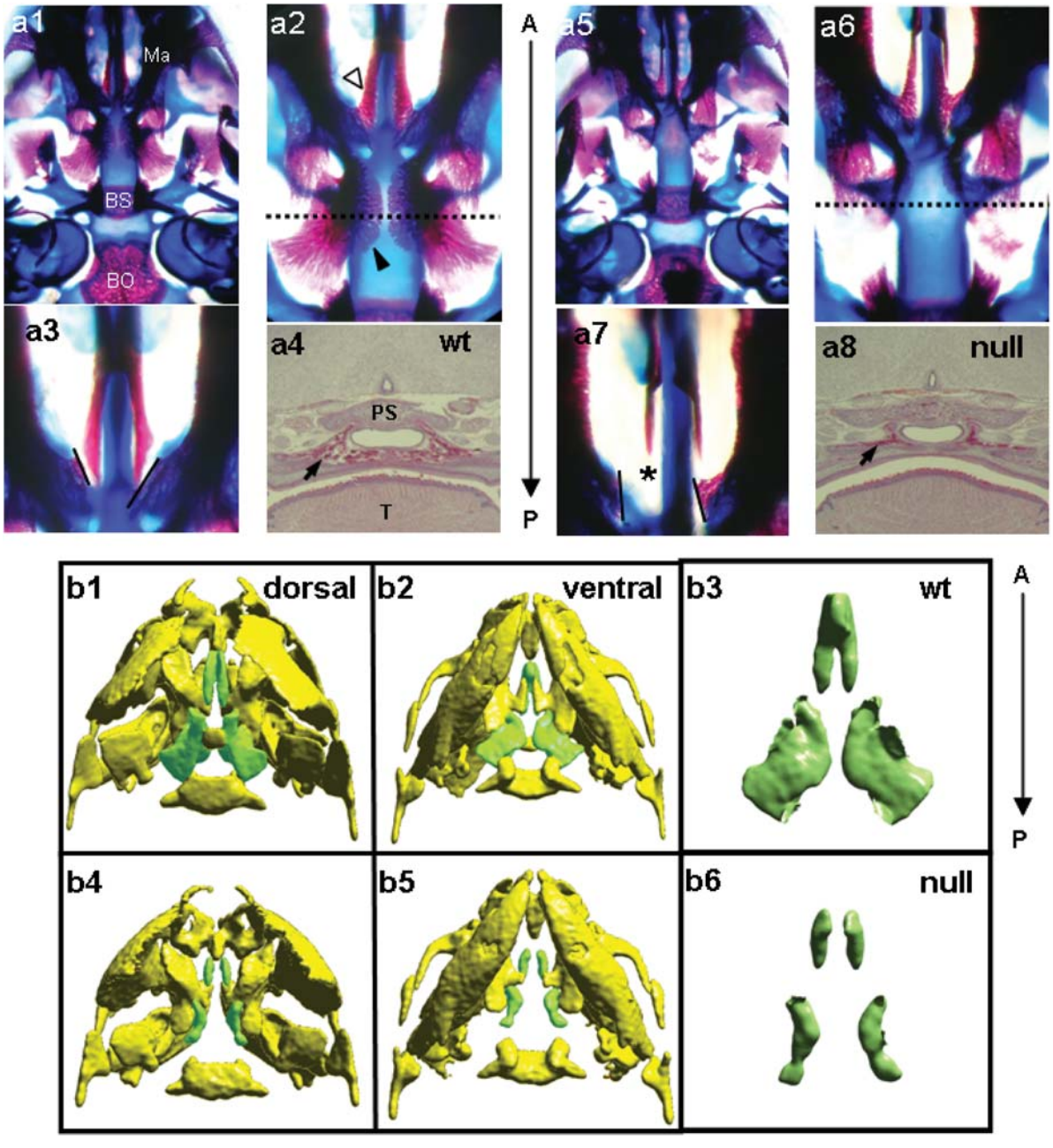

Figure 2. Loss of *Tbx22* causes bone phenotypes in the palate and vomer. (**A**) Ventral view of skeletal preparations with Alizarin Red (bone) and Alcian Blue (cartilage) of E18.5 embryos reveal reduced posterior palatal bones (black arrowhead), although anterior (maxillary) palatal bones (white arrowhead) are normal (a2,6). Additionally, the vomer is reduced (asterix in a7), visible after removing the maxillary palatine processes (black lines indicate cut surfaces). Coronal sections (a4,8; approximately at the level of the dotted lines in a2,6) stained with H&E show the mineralized palatine bone in wild-type embryos, although there is severely reduced mineralization in the $Tbx22^{null}$ embryo (black arrows). (**B**) Bone 3D surfaces generated from microCT scans of E18.5 day heads reveal the reduced size of the vomer and palatine bone (green). Occipital bone surfaces have been removed to facilitate dorsal view. BS = basisphenoid, BO = basoccipital, Ma = mandible, PS = presphenoid, T = tongue, A = anterior, *P* = posterior.

For all of the data presented in this study, the neo^{R} cassette is retained on the $Tbx22^{null}$ allele, however, no effects were attributable to its presence since identical phenotypes were also observed in mutants following *in vivo* excision with an Flp-deleter (data not shown). Similarly, the same spectrum of phenotypes and severity range was observed when the $Tbx22^{null}$ allele was crossed onto 129/SvJ and C57BL/6J strains and bred to >95% congenicity.

DISCUSSION

$Tbx22^{null}$ mice show multiple craniofacial defects that include submucous or overt CP, choanal atresia, reduced vomer and ankyloglossia, which are all consistent with its known expression pattern (12,18,19). Ankyloglossia was expected as it is a characteristic phenotype, frequently associated with CPX syndrome (8,9). Contrary to the variable penetrance in

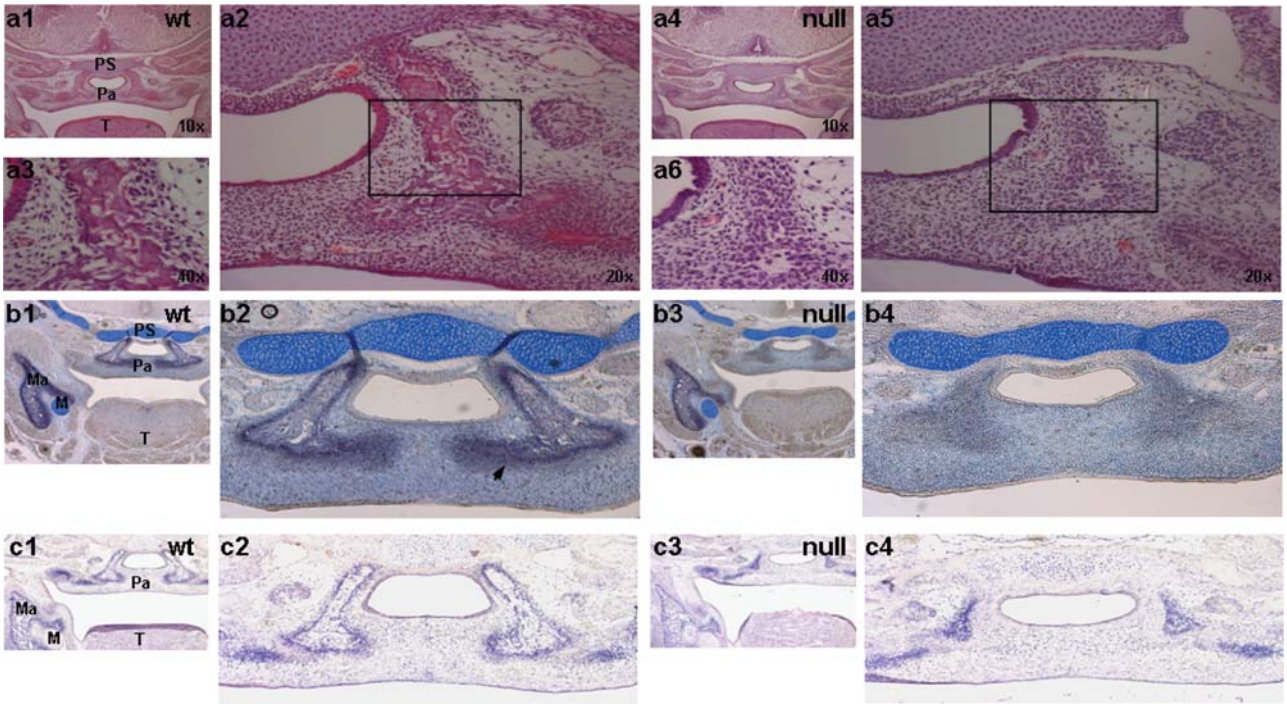

Figure 3. Reduced bone formation in the posterior hard palate is due to delayed maturation of osteoblasts. (**A**) H&E stained coronal sections of E15.5 embryos. In the wild-type, osteogenesis of the posterior palate is progressing normally with mineralized bone matrix visible (pink osteoid) on either end of the nasal passage (a1,2,3). In contrast, although condensation of mesenchyme can be observed in the *Tbx22*^{null}, mineralization is absent (a4,5,6). (**B**) Alkaline phosphatase activity assay on coronal sections of E15.5 embryos. In the wild-type, enzyme activity (purple) is observed in the osteoblasts on the edges of the posterior palatine osteogenic centre (arrow) (b1,2). In the *Tbx22*^{null}, alkaline phoshatase staining is severely reduced (b3,4). Sections are counter-stained with Alcian Blue. (**c**) *In situ* hybridization of coronal sections for *Runx2*. Expression can be detected in the developing mandible, palate and tooth buds in wild-type embryos (c1,2). *Tbx22*^{null} mutant embryos show reduced expression of *Runx2* in the posterior palate (c3,4). Ma = mandible, M = Meckel's cartilage, Pa = palate, PS = presphenoid, T = tongue.

CPX patients, this defect was detected in all *Tbx22*^{null} mice studied. The extent of the defect is variable but never as prominent or severe as that described in the *Lgr5* loss-of-function mutant (22). In these mice the defect is reported to be lethal, with null animals dying within 24 h of birth with empty, distended stomachs, filled with air. This is not unlike the *Tbx22*^{null} mice that fail to thrive except that the tongue defect is considerably milder. We suggest that other defects are more likely to be responsible for the prenatal demise observed.

Malformation of the vomer bone has not previously been discussed in relation to X-linked CP but has certainly been associated with both CP and SMCP. In a study of 30 patients undergoing surgery for SMCP, all were found to have vomerine malformations with the most frequently observed defect being a failure in vomer fusion with the rostral part of the palatal shelves (23). Similarly in a small series of fetuses the vomer was found to be poorly developed and also not fused in the region of the maxillary process in those with CP, which contrasted to the normal fetuses studied (24). We have not studied *Tbx22*^{null} mice at adult stages, but observations from around P12 also show the vomer to be severely underdeveloped. The vomer is thought to play a role in support of the secondary palate and also the development and separation of the choana. However, as choanal atresia is usually associated with a thickening of the vomer it may be more likely that these defects are independent (25). Nevertheless, the relevance of the vomer to SMCP and the pathology of VPI are currently unknown and in need of further investigation.

Our data, at least on the surviving *Tbx22*^{null} mice, suggests that they have an occult SMCP, where the palatal bone is affected, but the insertion of the palatine muscles into the aponeurosis, and the function of the palate, remains intact. Analysis of the posterior palatal bone has shown a distinct reduction of alkaline phoshatase in the development of the palatal bone, while expression of *Runx2* was intact at early stages, up to and including E14.5. Interestingly, TBX3 has recently been identified as a negative regulator of osteoblast differentiation in limb development with T-box binding sites identified in the regulatory regions of both *Runx2* and *Osterix* genes (26). Although we cannot exclude the possibility that the expression of *Runx2* is impaired by E15.5, the gross differences in palatal morphology between wild-type and mutant at this stage are already too large to make a direct comparison. These results therefore indicate a role for TBX22 in *Runx2*-independent and late differentiation of osteoblasts in the posterior palate. A delay of at least one embryonal day (as mirrored by the alkaline phoshatase expression) seems sufficient for a reduction in bone formation and function of the palate.

Whereas none of the craniofacial expressed genes we investigated were noticeably up or down regulated in *Tbx22*^{null} palates, we did observe an upregulation and broadening of the expression domain of *Pax9* throughout the persistent

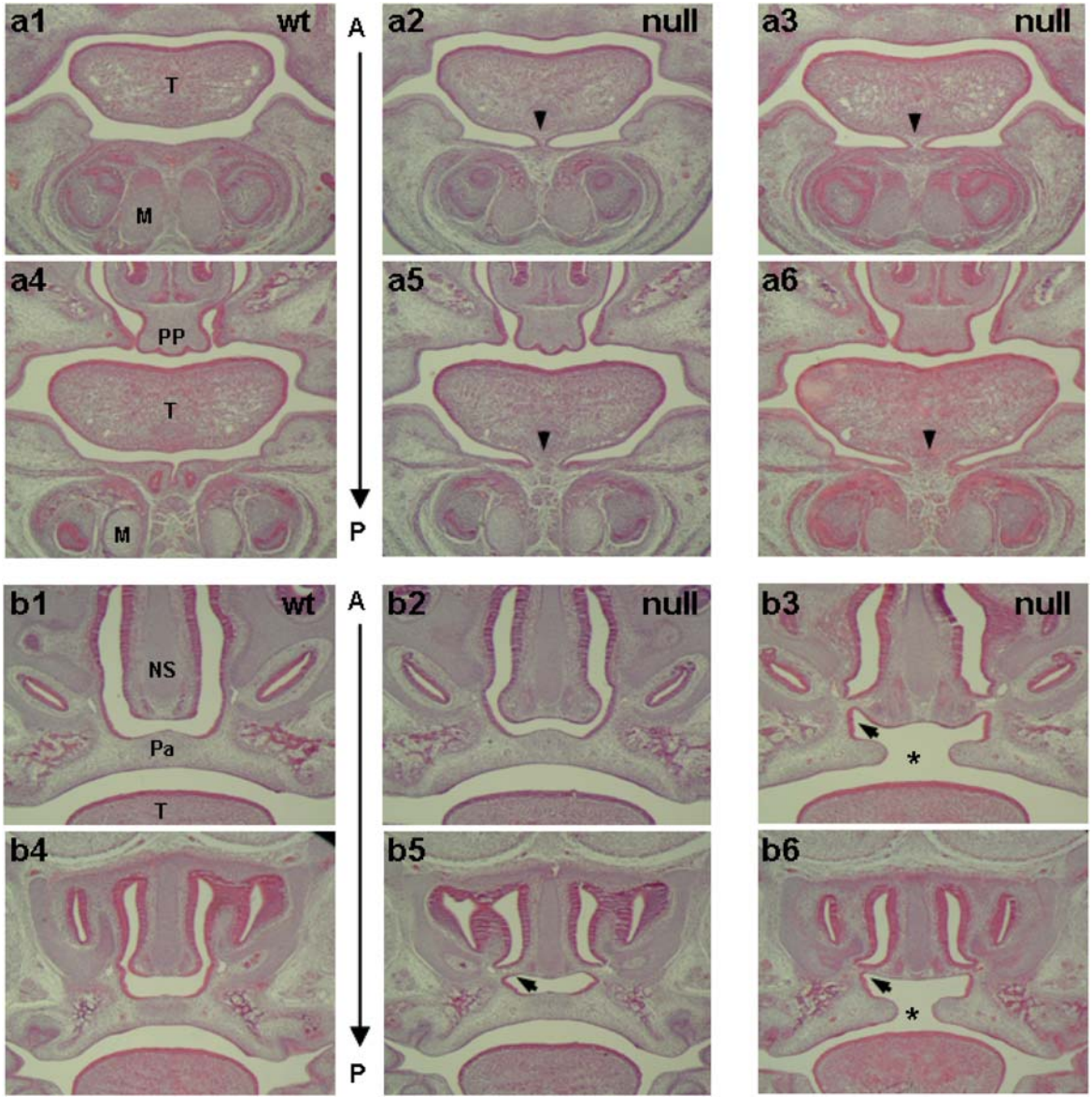

Figure 4. Phenotypic analysis of *Tbx22*^{null} mice. Embryos were collected at E15.5 and coronal sections were stained with H&E. (**A**) Ankyloglossia, or tongue-tie is observed in all mutant embryos (closed arrows in a2,3,5,6). In *Tbx22*^{null} mutants (a5,6), the tongue is usually attached caudally, at least as anteriorly as the incisive foramen, which is the transition between the primary and secondary palate, while at that point the tongue in the wild-type embryos is free (a4). (**B**) Choanal atresia is observed in mutant embryos with variable severity. In *Tbx22*^{null} embryos, a persistent oro-nasal membrane (arrows in b3,5,6) can be observed. M = Meckel's cartilage, NS = nasal septum, Pa = palate, PP = primary palate, T = tongue, A = anterior, *P* = posterior.

oro-nasal membrane. It is not yet clear if this is a direct effect, although both human and mouse *Pax9* promoters contain putative T-box binding sites in an area of sequence homology (>80%). Inappropriate expression of *Pax9* in the oro-nasal membrane could provide a possible explanation for its persistence since it is believed to promote cell survival, both by regulating the expression of genes involved in mediating cell proliferation and resistance to apoptosis (27). Although choanal atresia is not currently a recognized feature of CPX, this may in part be due to selection bias and will require specific investigation in the future. Choanal atresia has previously been described in combination with overt CP in CHARGE syndrome, which usually also includes other features such as coloboma, heart defects and growth restriction. About 60–80% of patients are estimated to be associated with haploinsufficiency of the gene *CHD7* (28) and mice mutant for this gene provides a useful model (29). Choanal atresia has also been described in the *Raldh3* null mouse mutant, which presents with a similar post-natal lethal respiratory distress phenotype, where the pups become cyanotic and die within 10 h (30). It is suggested that the persistence of the nasal fins may result from impairment to normal retinoic acid synthesis, which in turn down-regulates *Fgf8* expression in the nasal fins. The authors also demonstrate the prevention of choanal atresia using a maternal non-teratogenic dose of retinoic acid.

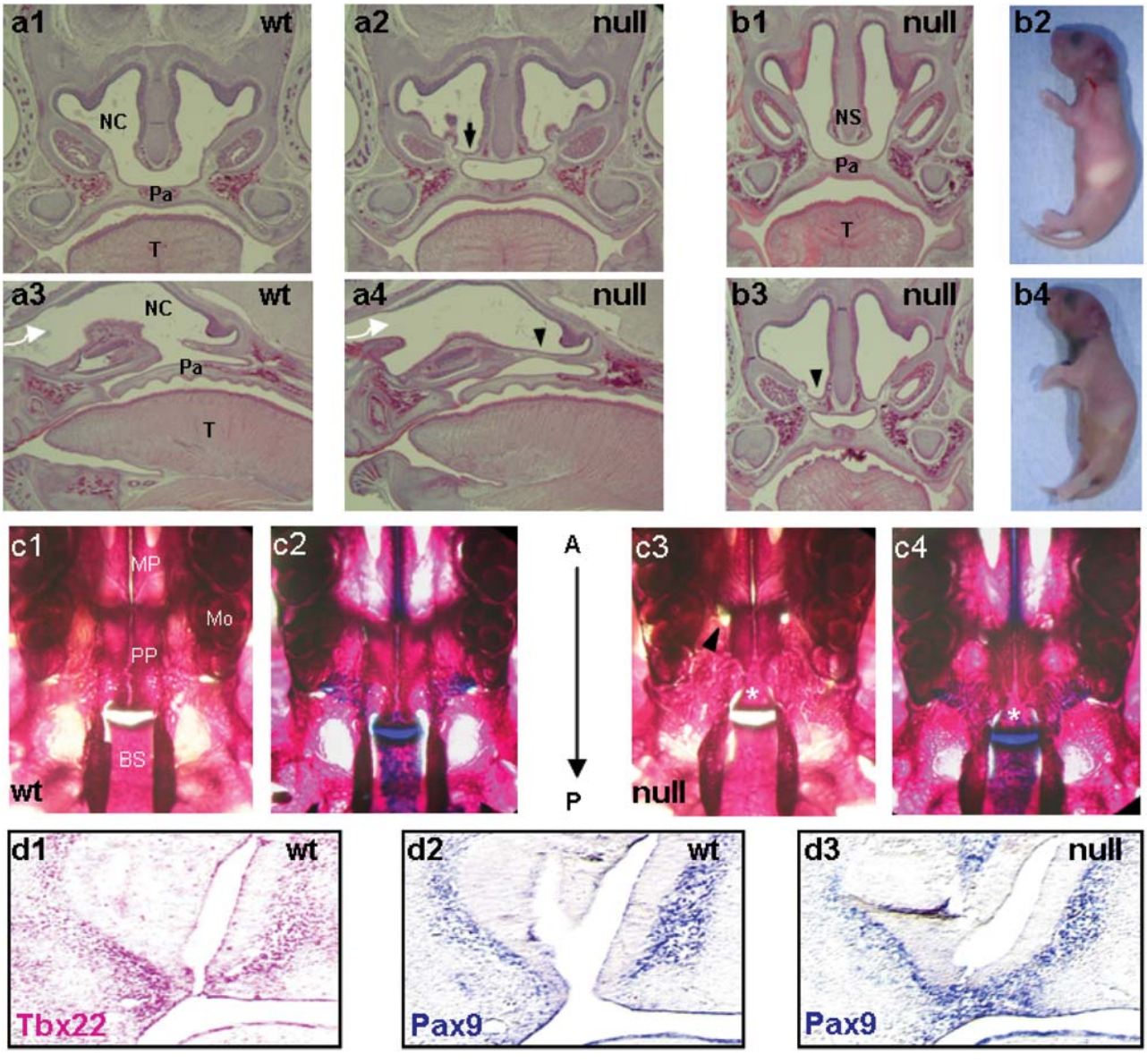

Figure 5. Choanal atresia is the likely cause of death in *Tbx22*^{null} mice. (**A**) In E18.5 embryos the choanal defect can be seen clearly in coronal (a1,2) as well as sagittal (a3,4) sections of the head. In the null animal (a2,4) the persistent oro-nasal membrane (black arrowhead) blocks the air-flow (white arrow) from the nostril into the oral pharynx and eventually the trachea. (**B**) When analyzing *Tbx22*^{null} littermates we observe that around half suckle successfully (b2), while the other half perish within 24 hours with breathing difficulties and air in the stomach (b4). (**C**) Skeletal preparations with Alizarin Red and/or Alcian Blue at postnatal day 12 in wild-type and *Tbx22*^{null} survivors show the extent of the submucous cleft as a notch in the posterior end of the hard palate at the cartilage between the basisphenoid and the presphenoid (asterisk). Palatine bone size is further reduced as is evident from the incomplete fusion with the maxillary part of the palatine bone (arrowhead). (**D**) *In situ* hybridizations showing expression of *Tbx22* (pink) and *Pax9* (blue) in lateral and medial nasal mesenchyme, either side of the choana. In *Tbx22*^{null} embryos, expression of *Pax9* can be observed in the persistent oro-nasal membrane. BS = basisphenoid, Mo = molar, MP = maxillary process, NC = nasal cavity, Pa = palate, PP = palatine process, T = tongue.

In contrast to many other CP mouse models where the specific genetic background had significant impact on either penetrance or severity, for example as described in the *Tgfb3* mutant (31), our analysis in CD1, 129Sv and C57Bl6 strains has shown similar phenotypes and with a similar penetrance for each. It is also interesting to note that unlike in the human, female heterozygote mutant mice are all unaffected whereas the null females are the same as male null animals. It will be interesting to determine whether these differences are due to additional genetic or environmental factors or differences in X-inactivation between mouse and human.

In summary, the *Tbx22*^{null} mouse has developmental defects similar to those found in patients with CPX and provides a new and unique model to understand the SMCP phenotype. Unlike overt clefts, this clinically recognizable form of SMCP has not been extensively studied in the mouse with only *Tshz1* and *Tgfbr2* mutants described with either cleft or premature truncation of the soft palate respectively (32,33). Both of these defects are restricted to soft palate development

and do not appear to involve the hard palate, which is a common cause of human SMCP. Since other mouse models for CP are frequently reported with less than 100% penetrance, our data suggests it might also be valuable to investigate the non-penetrant animals for intramembranous bone formation. The *Tbx22*^{null} model, clearly argues that SMCP is a continuous part of the same phenotypic spectrum. The precise molecular mechanism of the TBX22 transcriptional signaling cascade still remains to be determined but a failure in palatal osteoblast differentiation and maturation has been highlighted. A review of all CPX cases known to us suggests that SMCP is at least as common as overt CP (unpublished observations). This frequency might turn out to be even higher given a potential bias towards screening for *TBX22* mutations in overt CP cases. This study provides important new insight to further our understanding of common craniofacial birth defects and to initiate a proper exploration of the relationship between overt CP and SMCP.

MATERIALS AND METHODS

Generation of the *Tbx22*^{null} allele

The *Tbx22* targeting vector was generated by cloning genomic fragments, a loxP site and a loxP-frt-Neo-frt cassette into the pSP72 vector (Fig. 1A). The integrity of the targeting construct was confirmed by DNA sequencing. The vector was linearized and electroporated into 129/Sv embryonic stem (ES) cells (Kindly provided by E. Robertson). Successfully targeted G418 resistant clones were identified by PCR and confirmed by Southern blot analysis. Positive clones were used to generate chimera in C57BL/6J mice. Germline floxed mice (*Tbx22*$^{tm1(flox/exon0\text{-}2/NEO)Sta}$) were bred to β-actin-Cre mice to remove the first three exons and create a *Tbx22* deleted strain. This created the *Tbx22*$^{tm1.1(b\text{-}actin/Dexon0\text{-}2/NEO)Sta}$ allele, which we called *Tbx22*^{null}. Subsequently, mice were backcrossed onto CD1, 129/SvJ and C57BL/6J strains to >95% congenicity.

Histological analysis

Embryos were collected from *Tbx22*$^{+/-}$ females crossed with *Tbx22*$^{-/Y}$ males at different embryonic time points. Litters were dissected and fixed in 4% paraformaldehyde overnight. Embryos were paraffin-embedded, sectioned and stained with H&E. Alkaline phosphatase assay was performed by incubating deparaffinized sections with 0.5 mg/ml NBT/BCIP solution and counterstaining with Alcian Blue. Skeletal preparations were performed by removing the skin, fixing heads in 100% ethanol overnight, and staining in Alizarin Red and Alcian Blue solution, followed by clearing in 1% KOH for several days.

MicroCT imaging

Specimens were prepared and scanned as previously described (34). In brief, fixed fetuses were wrapped with a loose thin sponge and immersed in 1 × PBS in a plastic container then scanned on volumetric microCT scanner at 27 μm isometric voxel resolution using an eXplore Locus RS Small Animal MicroCT Scanner (GE Healthcare, London, ON, Canada). This volumetric scanner uses a 3500 × 1750 CCD detector for Feldkamp cone-beam reconstruction. The platform independent parameters of current, voltage and exposure time were kept constant at 450 μA, 80 kVP and 2000 ms, respectively. Additional scan parameters include 900 evenly spaced view angles (views) and 10 frames per view. Scan time was 400 min per sample. Images were reconstructed with the manufacturer's proprietary EVSBeam software. Images were analyzed and bone surfaces generated using Microview (version 2.0.29), ImageJ (version 1.41) and VAM (version 0.8.13).

In situ hybridization

For *in situ* hybridization, embryos were fixed overnight in 4% paraformaldehyde in PBS, dehydrated through graded alcohols, embedded in paraffin wax and sectioned at 8 μm thickness. Non-radioactive RNA *in situ* hybridization of tissue sections was performed as previously described (35). Dioxigenin-labeled *Tbx22* antisense riboprobe was generated with the *In vitro* Transcription kit (Roche Applied Science), and anti-digoxigenin-AP antibody (1 : 1000) (Roche Applied Science) was used to detect the hybridization signals.

URL

OMIM, http://www.ncbi.nlm.nih.gov/omim/.

SUPPLEMENTARY MATERIAL

Supplementary Material is available at *HMG* online.

ACKNOWLEDGEMENTS

We thank Massimo Signore (ES cell/chimera production service, UCL ICH), Zoe Webster and Jonathan Godwin (Transgenics and ES Cell laboratory, MRC/Imperial College London) for expert help with the generation of transgenic animals. We also thank Kit Doudney and James Grinham for technical assistance.

Conflict of Interest statement. None declared.

FUNDING

This work was supported by the Wellcome Trust [071494/Z/03/Z] and the Child Health Research Appeal Trust. Funding to pay the Open Access charge was provided by the Wellcome Trust.

REFERENCES

1. Murray, J.C. and Schutte, B.C. (2004) Cleft palate: players, pathways, and pursuits. *J. Clin. Invest.*, **113**, 1676–1678.
2. Stanier, P. and Moore, G.E. (2004) Genetics of cleft lip and palate: syndromic genes contribute to the incidence of non-syndromic clefts. *Hum. Mol. Genet.*, **13**, R73–R81.
3. Weatherley-White, R.C., Sakura, C.Y. Jr, Brenner, L.D., Stewart, J.M. and Ott, J.E. (1972) Submucous cleft palate. Its incidence, natural history, and indications for treatment. *Plast. Reconstr. Surg.*, **49**, 297–304.
4. Garcia, V.M., Ysunza, A., Hernandez, X. and Marquez, C. (1988) Diagnosis and treatment of submucous cleft palate: a review of 108 cases. *Cleft Palate J.*, **25**, 171–173.

5. Kelly, A.B. (1910) Congenital insufficiency of the palate. *J. Laryngol. Otol.*, **25**, 281–358.
6. Kaplan, E.N. (1975) The occult submucous cleft palate. *Cleft Palate J.*, **12**, 356–368.
7. Braybrook, C., Doudney, K., Marçano, A.C., Arnason, A., Bjornsson, A., Patton, M.A., Goodfellow, P.J., Moore, G.E. and Stanier, P. (2001) The T-box transcription factor gene TBX22 is mutated in X-linked cleft palate and ankyloglossia. *Nat. Genet.*, **29**, 179–183.
8. Marçano, A.C., Doudney, K., Braybrook, C., Squires, R., Patton, M.A., Lees, M.M., Richieri-Costa, A., Lidral, A.C., Murray, J.C., Moore, G.E. and Stanier, P. (2004) TBX22 mutations are a frequent cause of cleft palate. *J. Med. Genet.*, **41**, 68–74.
9. Suphapeetiporn, K., Tongkobpetch, S., Siriwan, P. and Shotelersuk, V. (2007) TBX22 mutations are a frequent cause of non-syndromic cleft palate in the Thai population. *Clin. Genet.*, **72**, 478–483.
10. Pauws, E. and Stanier, P. (2008) Epstein, C.J., Erickson, R.P. and Wynshaw-Boris, A. (eds), *Inborn Errors of Development*. Oxford University Press, New York, pp. 878–882.
11. Pauws, E. and Stanier, P. (2007) FGF signalling and SUMO modification: new players in the aetiology of cleft lip and/or palate. *Trends Genet.*, **23**, 631–640.
12. Braybrook, C., Lisgo, S., Doudney, K., Henderson, D., Marçano, A.C., Strachan, T., Patton, M.A., Villard, L., Moore, G.E., Stanier, P. and Lindsay, S. (2002) Craniofacial expression of human and murine TBX22 correlates with the cleft palate and ankyloglossia phenotype observed in CPX patients. *Hum. Mol. Genet.*, **11**, 2793–2804.
13. Andreou, A.M., Pauws, E., Jones, M.C., Singh, M.K., Bussen, M., Doudney, K., Moore, G.E., Kispert, A., Brosens, J.J. and Stanier, P. (2007) TBX22 missense mutations found in X-linked cleft palate (CPX) patients affect DNA binding, sumoylation and transcriptional repression. *Am. J. Hum. Genet.*, **81**, 700–712.
14. Pauws, E., Moore, G.E. and Stanier, P. (2009) A functional haplotype variant in the *TBX22* promoter is associated with cleft palate and ankyloglossia. *J. Med. Genet.*, **46**, 555–561.
15. Beaster-Jones, L., Horton, A.C., Gibson-Brown, J.J., Holland, N.D. and Holland, L.Z. (2006) The amphioxus T-box gene, AmphiTbx15/18/22, illuminates the origins of chordate segmentation. *Evol. Dev.*, **8**, 119–129.
16. Bush, J.O., Lan, Y. and Jiang, R. (2004) The cleft lip and palate defects in Dancer mutant mice result from gain of function of the Tbx10 gene. *Proc. Natl. Acad. Sci. U. S. A.*, **101**, 7022–7027.
17. Jerome, L.A. and Papaioannou, V.E. (2001) DiGeorge syndrome phenotype in mice mutant for the T-box gene, Tbx1. *Nat. Genet.*, **27**, 286–291.
18. Bush, J.O., Lan, Y., Maltby, K.M. and Jiang, R. (2002) Isolation and Developmental Expression Analysis of Tbx22, the Mouse Homolog of the Human X-linked Cleft Palate Gene. *Dev. Dyn.*, **225**, 322–326.
19. Haenig, B., Schmidt, C., Kraus, F., Pfordt, M. and Kispert, A. (2002) Cloning and expression analysis of the chick ortholog of TBX22, the gene mutated in X-linked cleft palate and ankyloglossia. *Mech. Dev.*, **117**, 321–325.
20. Proetzel, G., Pawlowski, S.A., Wiles, M.V., Yin, M., Boivin, G.P., Howles, P.N., Ding, J., Ferguson, M.W. and Doetschman, T. (1995) Transforming growth factor-beta 3 is required for secondary palate fusion. *Nat. Genet.*, **11**, 409–414.
21. Schroeder, T.M., Jensen, E.D. and Westendorf, J.J. (2005) Runx2: a master organizer of gene transcription in developing and maturing osteoblasts. *Birth Defects Res. C. Embryo. Today*, **75**, 213–225.
22. Morita, H., Mazerbourg, S., Bouley, D.M., Luo, C.W., Kawamura, K., Kuwabara, Y., Baribault, H., Tian, H. and Hsueh, A.J. (2004) Neonatal lethality of LGR5 null mice is associated with ankyloglossia and gastrointestinal distension. *Mol. Cell. Biol.*, **24**, 9736–9743.
23. Grzonka, M.A., Koch, K.H., Koch, J. and Glindemann, S. (2001) Malformation of the vomer in submucous cleft palate. *J. Craniomaxillofac. Surg.*, **29**, 106–110.
24. Hansen, L., Nolting, D., Holm, G., Hansen, B.F. and Kjaer, I. (2004) Abnormal vomer development in human fetuses with isolated cleft palate. *Cleft Palate Craniofac. J.*, **41**, 470–473.
25. Molina-Martinez, C., Guilemany-Toste, J.M., Cervera-Escario, J. and Bernal-Sprekelsen, M. (2009) Stucker, F., de Souza, C., Kenyon, G., Lian, T., Draf, W. and Schick, B. (Eds), *Rhinology and Facial Plastic Surgery*. Springer, Berlin Heidelberg, pp. 685–690.
26. Govoni, K.E., Linares, G.R., Chen, S.T., Pourteymoor, S. and Mohan, S. (2009) T-box 3 negatively regulates osteoblast differentiation by inhibiting expression of osterix and runx2. *J. Cell. Biochem.*, **106**, 482–490.
27. Robson, E.J.D., He, S.-J. and Eccles, M.R. (2006) A PANorama of PAX genes in cancer and development. *Nat. Rev. Cancer*, **6**, 52–62.
28. Vissers, L.E., van Ravenswaaij, C.M., Admiraal, R., Hurst, J.A., de Vries, B.B., Janssen, I.M., van der Vliet, W.A., Huys, E.H., de Jong, P.J., Hamel, B.C. *et al.* (2004) Mutations in a new member of the chromodomain gene family cause CHARGE syndrome. *Nat. Genet.*, **36**, 955–957.
29. Bosman, E.A., Penn, A.C., Ambrose, J.C., Kettleborough, R., Stemple, D.L. and Steel, K.P. (2005) Multiple mutations in mouse Chd7 provide models for CHARGE syndrome. *Hum. Mol. Genet.*, **14**, 3463–3476.
30. Dupe, V., Matt, N., Garnier, J.M., Chambon, P., Mark, M. and Ghyselinck, N.B. (2003) A newborn lethal defect due to inactivation of retinaldehyde dehydrogenase type 3 is prevented by maternal retinoic acid treatment. *Proc. Natl. Acad. Sci. U. S. A.*, **100**, 14036–14041.
31. Martinez-Sanz, E., Del, R.A., Barrio, C., Murillo, J., Maldonado, E., Garcillan, B., Amoros, M., Fuerte, T., Fernandez, A., Trinidad, E. *et al.* (2008) Alteration of medial-edge epithelium cell adhesion in two Tgf-beta3 null mouse strains. *Differentiation*, **76**, 417–430.
32. Core, N., Caubit, X., Metchat, A., Boned, A., Djabali, M. and Fasano, L. (2007) Tshz1 is required for axial skeleton, soft palate and middle ear development in mice. *Dev. Biol.*, **308**, 407–420.
33. Xu, X., Han, J., Ito, Y., Bringas, P. Jr, Urata, M.M. and Chai, Y. (2006) Cell autonomous requirement for Tgfbr2 in the disappearance of medial edge epithelium during palatal fusion. *Dev. Biol.*, **297**, 238–248.
34. Vasquez, S.X., Hansen, M.S., Bahadur, A.N., Hockin, M.F., Kindlmann, G.L., Nevell, L., Wu, I.Q., Grunwald, D.J., Weinstein, D.M., Jones, G.M. *et al.* (2008) Optimization of volumetric computed tomography for skeletal analysis of model genetic organisms. *Anat. Rec. (Hoboken)*, **291**, 475–487.
35. Wilkinson, D.G. (1998) *In Situ Hybridization: A Practical Approach*. IRL Press, Oxford.